Journal of Alloys and Compounds 504S (2010) S34–S37

Contents lists available at ScienceDirect

Journal of Alloys and Compounds

journal homepage: www.elsevier.com/locate/jallcom

# Co–B–Si–Ta bulk metallic glasses designed using cluster line and alloying

C.L. Zhu, Q. Wang, Y.M. Wang, J.B. Qiang, C. Dong*

*Key Lab of Materials Modification (Ministry of Education), Dalian University of Technology, Dalian 116024, China*

ARTICLE INFO

*Article history:*
Received 30 June 2009
Received in revised form 29 March 2010
Accepted 13 April 2010
Available online 20 April 2010

*Keywords:*
Amorphous materials
Clusters
Casting
Thermal analysis

ABSTRACT

The formations of Co-based Co–B–Si–Ta bulk metallic glasses, as well as their mechanical and corrosion properties have been explored in this work. The alloy compositions were designed by using the cluster line approach and the alloying strategy, where the cluster line referred to a straight composition line linking a specific binary cluster to the third element in a ternary alloy phase diagram. The base ternary compositions in the Co–B–Si ternary system were first determined by the intersection points of two cluster lines, Co–B cluster to Si and Co–Si cluster to B. Then these basic ternary compositions were a small amount of Ta alloyed to further improve the glass-forming abilities. Experimental results revealed that good glass formers with 4 mm in diameter occurred at $Co_{62.2}B_{26.9}Si_{6.9}Ta_4$, obtained by Ta alloying of the base intersection compositions of $Co_7B_3$–Si with $Co_9Si$–B. This bulk metallic glass have not only high thermal stabilities with high $T_g$ and $T_x$ values, but also exhibit high fracture strength of about 4760 MPa, high Vickers hardness of about 1460, a Young's modulus of 198 GPa, and good corrosion resistances in 1 mol/L HCl and 3 mass% NaCl solutions.



## 1. Introduction

Since the work by Duwez and his coworkers in 1960 [1], a large number of metallic glasses have been developed as potential structural and functional materials. Among these alloys, Co-based bulk metallic glasses (BMGs) have been investigated due to their high strength, excellent soft magnetic and corrosion properties [2–5]. Such as, the highest fracture strength reached as high as 5185 MPa for Co–Fe–B–Ta alloy [5]. They generally exhibit large glass-forming abilities (GFAs) only in multi-component alloy systems, such as $Co_{48}Cr_{15}Mo_{14}C_{15}B_6Er_2$, and the maximum size of the formed BMGs reaches 10 mm in diameter [6]. However, it is very difficult to search for good BMG formers in so complex multi-component alloy systems. Many empirical guidelines, including three empirical rules [2], confusion principle [7], eutectic [8], and minor alloying strategy [9], etc., have been proposed to solve this question. In our previous works, we used the concept of short-range order, characterized by 1st-shell coordination polyhedra, to propose a cluster line approach, which has been applied successfully for the composition design of Zr-, Cu-, RE- (RE, Rare Earth) Ni- and Fe-based alloys [10–13]. This approach greatly simplifies the traditional trial-and-error method in producing good glass formers.

In the present work, we will attempt to develop Co-based Co–B–Si–Ta BMG compositions through a combination of the cluster line approach with a small amount of Ta alloying strategy. Basic ternary compositions of Co–B–Si are first determined by the intersection points of two cluster lines, Co–B cluster to Si and Co–Si cluster to B, and then alloyed with a fourth element Ta to improve GFAs. The glass formation of these compositions is investigated by means of copper mould suction casting. The mechanical and corrosion properties of Co-based BMGs are also investigated.

## 2. Composition design

The so-called cluster line in a ternary phase diagram is defined as a straight composition line linking a binary atomic cluster composition to the third element. The specific binary clusters are nearest neighbour coordination polyhedra derived from binary crystalline phases that are related with a eutectic reaction [13].

The formation of metallic glasses is closely related with eutectic compositions [8]. It is believed that the local cluster structures in metallic glasses are similar to those in competing crystalline phases [14,15]. In the present work, the cluster for a cluster line is derived from a local structure of a eutectic phase. Large negative enthalpies of mixing between the constituent elements favor stable cluster structures. In the Co–B–Si system, the enthalpies of mixing of Co–B, Co–Si and B–Si are respectively $\Delta H^{mix}_{Co-B} = -24$ kJ/mol, $\Delta H^{mix}_{Co-Si} = -38$ kJ/mol and $\Delta H^{mix}_{B-Si} = -14$ kJ/mol [16]. The $\Delta H$ of Co–B and Co–Si pairs are negatively larger than that of B–Si pair and the aim of design Co-based alloys, so the Co–B and Co–Si eutectic phases are considered to select the clusters.

* Corresponding author. Tel.: +86 411 84708389; fax: +86 411 84708389.
*E-mail address:* dong@dlut.edu.cn (C. Dong).

0925-8388/$ – see front matter © 2010 Elsevier B.V. All rights reserved.
doi:10.1016/j.jallcom.2010.04.065

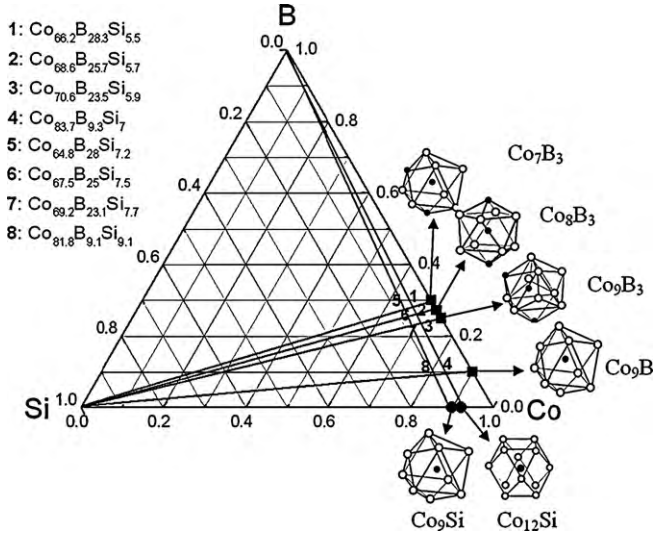


**Fig. 1.** Schematic composition chart of Co–B–Si ternary system. Cluster lines and intersection points are shown.

The Co–B eutectic phases CoB, $Co_2B$ and $Co_3B$ are characterized with two groups of clusters centered by small B atom, CN10 Archimedean octahedral antiprism $Co_8B_3$ and capped trigonal prisms with different CNs (coordination numbers): CN9 $Co_7B_3$ and $Co_9B$, CN11 $Co_9B_3$. Similarly, the Co-rich Co–Si eutectic phases $Co_3Si$ and $Co_2Si$ are respectively characterized by a CN12 cube-octahedron $Co_{12}Si$ and CN9 capped trigonal prism $Co_9Si$, both centered by Si. Therefore, six cluster lines, $Co_7B_3$–Si, $Co_8B_3$–Si, $Co_9B_3$–Si, $Co_9B$–Si $Co_{12}Si$-B and $Co_9Si$-B are constructed in the basic ternary Co–B–Si system, as shown in Fig. 1 like reference [14]. The Co–B cluster lines and Co–Si cluster lines intersect at eight basic ternary compositions $Co_{66.2}B_{28.3}Si_{5.5}$, $Co_{68.6}B_{25.7}Si_{5.7}$, $Co_{70.6}B_{23.5}Si_{5.9}$, $Co_{83.7}B_{9.3}Si_7$, $Co_{64.8}B_{28}Si_{7.2}$, $Co_{67.5}B_{25}Si_{7.5}$, $Co_{69.2}B_{23.1}Si_{7.7}$, $Co_{81.1}B_{9.1}Si_{9.1}$ Then 4 at.% Ta is added to these basic ternary composition alloys to investigate the BMG formation.

### 3. Experimental

Ingots of ternary Co–B–Si and quaternary Co–B–Si–Ta are prepared by using arc melting mixtures of constituent elements under high purity argon atmosphere. The purities of elements are 99.99 wt.% for Co, Si and Ta, 99.5 wt.% for B, respectively. Alloy rods with 2, 3 and 4 mm in diameter and 40 mm in length were prepared using copper mould suction casting method. Structural identification was carried out using X-ray diffractometry (XRD) with Cu-$K_\alpha$ radiation. A TA Q600 SDT differential thermal analyzer was employed to examine the thermal stabilities of the as-cast BMGs at a heating rate of 0.33 K/s. Vickers hardness was measured with a Vickers hardness tester under a load of 1.96 N. Mechanical properties, including Young's modulus ($E$) and fracture strength ($\sigma_f$) were measured by compression in an Instron testing machine. The gauge size was 2 mm in diameter and 4 mm in length, and the strain rate was $5 \times 10^{-4} s^{-1}$. Electrolytes of 3 mass% NaCl and 1 mol/L HCl solutions open to air were used for standard corrosion testing at room temperature. The sample weights before and after the corrosion tests were measured with an accuracy of $\pm 5 \times 10^{-6}$ g. Potentiodynamic polarization measurements were conducted in a typical three-electrode electrochemical cell with saturated calomel as the reference electrode and a platinum sheet as the counter electrode at room temperature, and the curves were measured with a potential sweep rate of 50 mV/min.

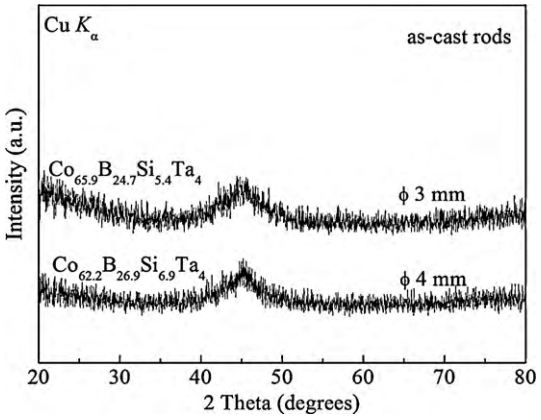


**Fig. 2.** XRD patterns of the Co-based BMGs.

### 4. Results and discussion

XRD results show that the designed ternary composition alloys cannot form amorphous rods due to weak GFAs. The 4 at.% Ta alloying of the basic ternary compositions should improve the GFAs of alloys as have been confirmed previously [13]. Several quaternary alloys could form 2 mm BMG rods. These BMG compositions are respectively $Co_{63.6}B_{27.2}Si_{5.2}Ta_4$, $Co_{65.9}B_{24.7}Si_{5.4}Ta_4$, $Co_{67.8}B_{22.6}Si_{5.6}Ta_4$, $Co_{62.2}B_{26.9}Si_{6.9}Ta_4$ and $Co_{64.8}B_{24}Si_{7.2}Ta_4$, where the basic compositions are intersections of cluster lines $Co_7B_3$–Si and $Co_{12}$Si-B (No. 1 in Fig. 1), $Co_8B_3$–Si and $Co_{12}$Si-B (No. 2), $Co_9B_3$–Si and $Co_{12}$Si-B (No. 3), $Co_7B_3$–Si and $Co_9$Si-B (No. 5), and $Co_8B_3$–Si and $Co_9$Si-B (No. 6), respectively. In order to check the GFAs of these BMGs, larger-size alloy rods with 3 mm and 4 mm in diameters were further prepared. The alloy $Co_{65.9}B_{24.7}Si_{5.4}Ta_4$ formed Ø 3 mm BMG rod and Ø 4 mm for another composition $Co_{62.2}B_{26.9}Si_{6.9}Ta_4$. Fig. 2 gives the XRD patterns of these two relatively large-size BMGs. It can be seen that the basic ternary compositions of these two BMGs are respectively the intersection points of CN10–CN12 and CN9–CN9 cluster lines (Nos. 2 and 5 in Fig. 1). It is interesting to notice that the former one coincides with the clusters of quasicrystals [17]. From these intersection rules, we can conclude that the best glass formers are generally classified into two types: one is based on CN9 capped trigonal prisms and the other on the combination of CN10 and CN12 polyhedra.

Table 1 lists the thermal parameters of Ø 2 mm BMGs, including $T_g$, $T_x$, $T_m$, $T_l$, $\Delta T_x$, $T_g/T_l$, $\gamma$, $H_v$, $E$ and $\sigma_f$, which are obtained from the DTA curves and compression test, It is found that these BMGs have high $T_g$ and $T_x$ values, and hence possess high thermal stabilities. The mechanical properties of $Co_{62.2}B_{26.9}Si_{6.9}Ta_4$ and $Co_{65.9}B_{24.7}Si_{5.4}Ta_4$ were investigated. The Vickers hardnesses $H_v$ of these two BMGs are respectively 1461 and 1440. Their compressive stress–stain curves (Fig. 4) exhibit brittle fracture and practically no plastic strain due to strong bonding forces among the constituent consistent with previous results [5]. The Young's modulus $E$ and fracture strength $\sigma_f$ of these two BMGs are 193 and 198 GPa; 4670 and 4760 MPa, respectively.

Corrosion assessments of the $Co_{62.2}B_{26.9}Si_{6.9}Ta_4$ and $Co_{65.9}B_{24.7}Si_{5.4}Ta_4$ BMGs were done by measuring the mass

**Table 1**
Compositions of Co-based BMGs and their experimental results. The compositions are expressed in two different ways.

| Experimental BMGs (at.%) | $T_g$ (K) | $T_x$ (K) | $T_m$ (K) | $T_l$ (K) | $\Delta T_x$ | $T_g/T_l$ | $\gamma$ | $H_v$ | $E$ (GPa) | $\sigma_f$ (MPa) |
|---|---|---|---|---|---|---|---|---|---|---|
| $Co_{63.6}B_{27.2}Si_{5.2}Ta_4$ ($Co_{66.2}B_{28.3}Si_{5.5})_{96}Ta_4$ | 873 | 917 | 1379 | 1418 | 44 | 0.616 | 0.400 | 1450 | 195 | 4590 |
| $Co_{65.9}B_{24.7}Si_{5.4}Ta_4$ ($Co_{68.6}B_{25.7}Si_{5.7})_{96}Ta_4$ | 866 | 909 | 1359 | 1422 | 43 | 0.609 | 0.397 | 1440 | 193 | 4670 |
| $Co_{67.8}B_{22.6}Si_{5.6}Ta_4$ ($Co_{70.6}B_{23.5}Si_{5.9})_{96}Ta_4$ | 837 | 882 | 1326 | 1435 | 45 | 0.583 | 0.388 | 1460 | 190 | 4620 |
| $Co_{62.2}B_{26.9}Si_{6.9}Ta_4$ ($Co_{64.8}B_{28}Si_{7.2})_{96}Ta_4$ | 896 | 933 | 1344 | 1426 | 37 | 0.628 | 0.402 | 1461 | 198 | 4760 |
| $Co_{64.8}B_{24}Si_{7.2}Ta_4$ ($Co_{67.5}B_{25}Si_{7.5})_{96}Ta_4$ | 872 | 912 | 1381 | 1417 | 40 | 0.615 | 0.398 | 1438 | 195 | 4580 |

**Table 2**
Corrosion potential ($E_{corr}$), Corrosion current density ($I_{corr}$) and Corrosion rate ($R_{corr}$) in 1 mol/L HCl and 3 wt.% NaCl solutions, respectively, at 298 K open to air for $Co_{62.2}B_{26.9}Si_{6.9}Ta_4$ and $Co_{65.9}B_{24.7}Si_{5.4}Ta_4$ BMG compositions.

| Electrolyte | Experimental BMGs (at.%) | $E_{corr}$ (V) | $I_{corr}$ ($10^{-2}$ A m$^{-2}$) | $R_{corr}$ ($10^{-3}$ mm/year) |
|---|---|---|---|---|
| 1 mol/L HCl | $Co_{62.2}B_{26.9}Si_{6.9}Ta_4$ | −0.131 | 5.6 | 5.3 |
| | $Co_{65.9}B_{24.7}Si_{5.4}Ta_4$ | −0.206 | 3.5 | 6.0 |
| | $Co_{43}Fe_{20}B_{31.5}Ta_{5.5}$ [18] | – | – | 13 |
| 3 mass% NaCl | $Co_{62.2}B_{26.9}Si_{6.9}Ta_4$ | −0.222 | 3.1 | 6.3 |
| | $Co_{65.9}B_{24.7}Si_{5.4}Ta_4$ | −0.369 | 1.7 | 6.9 |
| | $Co_{43}Fe_{20}B_{31.5}Ta_{5.5}$ [18] | – | – | 5.6 |

loss after the immersion test for 168 h at room temperature. Fig. 3(a) and (b) give potentiodynamic polarization curves of these two BMGs in 3 mass% NaCl and 1 mol/L HCl solutions respectively. Table 2 lists the measured corrosion rates $R_{corr}$, the corrosion potential $E_{corr}$ and the corrosion current density $I_{corr}$. The curve of $Co_{65.9}B_{24.7}Si_{5.4}Ta_4$ exhibits active dissolution prior to passivation, and the other curve shows a wide passive region in 1 mol/L HCl solution. In 3 mass% NaCl solution, however, these two BMGs are spontaneously passivated with a wide passive region, which indicate that these two BMGs have good corrosion resistances. Moreover, the corrosion-resistance property of the $Co_{62.2}B_{26.9}Si_{6.9}Ta_4$ BMG is superior to that of $Co_{65.9}B_{24.7}Si_{5.4}Ta_4$. The $E_{corr}$, $I_{corr}$ and $R_{corr}$ of the $Co_{62.2}B_{26.9}Si_{6.9}Ta_4$ BMG are respectively −0.131 V, $5.6 \times 10^{-2}$ A m$^{-2}$ and $5.3 \times 10^{-3}$ mm/year. In addition, the $R_{corr}$ values of these Co-based BMGs are consistent with a $Co_{43}Fe_{20}B_{31.5}Ta_{5.5}$ BMG reported in [18], all of them possessing high corrosion-resistance properties.

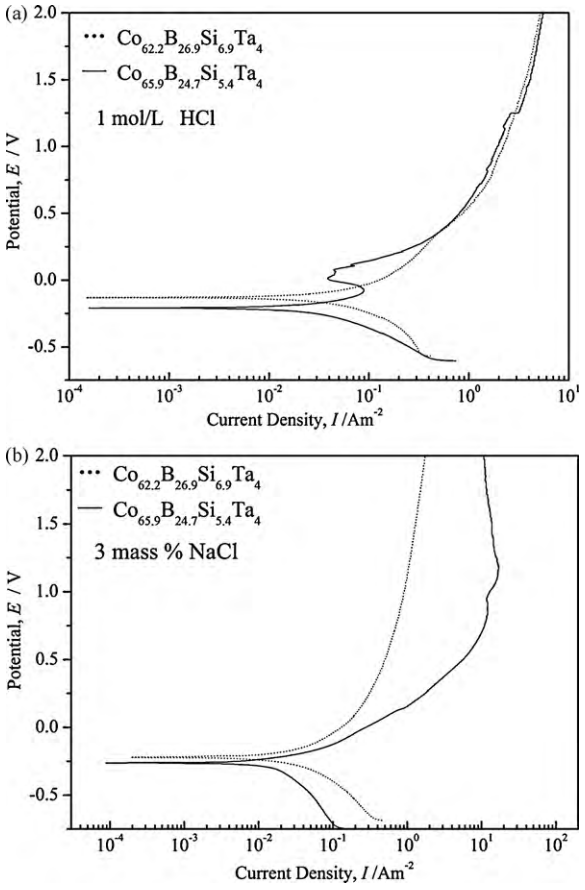


**Fig. 3.** (a) Potentiodynamic polarization curve of Co-based BMGs rods in 1 mol/L HCl solution open air at 298 K. (b) Potentiodynamic polarization curve of Co-based BMGs rods in 3% NaCl solution open air at 298 K.

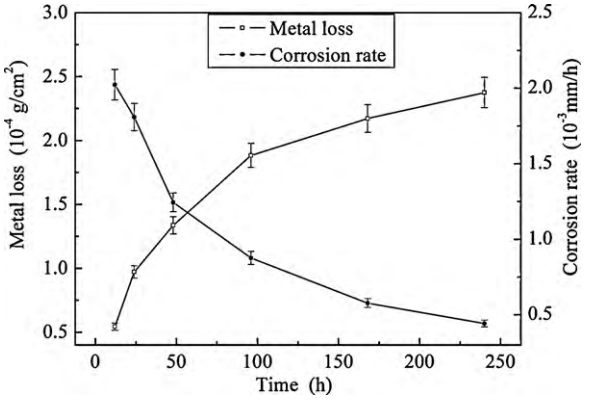


**Fig. 4.** Weight loss and the corresponding corrosion rate with time of $Co_{62.2}B_{26.9}Si_{6.9}Ta_4$.

The static immersion corrosion weight losses and the corrosion rates of the two BMGs were also measured. Fig. 4 shows the weight loss and corrosion rate of the $Co_{62.2}B_{26.9}Si_{6.9}Ta_4$ BMG in the 1 mol/L HCl solution as a function of time. The variation trend of corrosion loss versus time indicated that the corrosion rate was significant at the initial stage, and then was reduced to a low value at prolonged immersion time and the average corrosion rate is about 0.0039 mm/year.

## 5. Conclusions

Co–B–Si–Ta bulk metallic glasses are obtained by a combination of the cluster line approach with alloying principle. Ternary basic compositions in Co–B–Si system were first determined by the intersection points of two cluster lines. Then 4 at.% Ta alloying of the basic compositions improved the glass-forming abilities and a series of bulk metallic glass compositions were obtained. Among them, $Co_{62.2}B_{26.9}Si_{6.9}Ta_4$ possess large glass-forming abilities and can form Ø 4 mm amorphous rod. Furthermore, these two bulk metallic glasses exhibit high Vickers hardness of about 1500, good compressive properties with a fracture strength of about 4700 MPa, and good corrosion resistances with the corrosion rates of about $5.5 \times 10^{-3}$ mm/year and $6.5 \times 10^{-3}$ mm/year in 1 mol/L HCl and 3 mass% NaCl solutions, respectively.

## Acknowledgements

This project is supported by the National Science Foundation of China (No. 50671018, 50901012 and 50631010), the National Basic Research Program of China (No. 2007CB613902), and the Hi-Tech Research and Development Program of China (No. 2007AA05Z102).

## References

[1] W. Klement, R.H. Willens, P. Duwez, Nature 187 (1960) 869–870.
[2] A. Inoue, Acta Mater. 48 (2000) 279–306.

[3] A. Inoue, H. Koshiba, T. Itoi, A. Makino, Ferromagnetic, Appl. Phys. Lett. 73 (1998) 744–746.
[4] T. Itoi, A. Inoue, Mater. Trans. JIM 41 (2000) 1256–1262.
[5] A. Inoue, B.L. Shen, H. Koshiba, H. Kato, A.R. Yavari, Acta Mater. 52 (2004) 1631–1637.
[6] H. Men, S.J. Pang, T. Zhang, J. Mater. Res. 21 (2006) 958–961.
[7] A.L. Greer, Science 267 (1995) 1947–1953.
[8] D. Turnbull, Contemporary Phys. 10 (1969) 473–488.
[9] Z.P. Lu, C.T. Liu, Acta Mater. 50 (2002) 3501–3512.
[10] Q. Wang, J.B. Qiang, Y.M. Wang, J.H. Xia, X.F. Zhang, C. Dong, Intermetallics 12 (2004) 1229–1232.
[11] J. Wu, Q. Wang, J.B. Qiang, F. Chen, C. Dong, Y.M. Wang, C.H. Shek, J. Mater. Res. 22 (2007) 573–577.
[12] J.H. Xia, J.B. Qiang, Y.M. Wang, Q. Wang, C. Dong, Appl. Phys. Lett. 88 (2006) 101907.
[13] Q. Wang, C.L. Zhu, Y.H. Li, X. Cheng, W.R. Chen, J. Wu, J.B. Qiang, Y.M. Wang, C. Dong, J. Mater. Res. 23 (2008) 1543.
[14] P.H. Gaskell, Nature 276 (1978) 484–485.
[15] D.B. Miracle, J. Non-Cryst. Solids 342 (2004) 89–96.
[16] A. Takeuchi, A. Inoue, Mater. Trans. JIM 41 (2000) 1372–1378.
[17] C. Dong, Q. Wang, J.B. Qiang, Y.M. Wang, N. Jiang, G. Han, Y.H. Li, J. Wu, J.H. Xia, J Phys. D: Appl. Phys. 40 (2007) R273–R291.
[18] B.L. Shen, S.J. Pang, T. Zhang, H. Kimura, J. Alloys Comp. 460 (2008) L11–L13.